

# Electric field driven quantum phase transition between band insulator and topological insulator

Jun Li and Kai Chang

SKLSM, Institute of Semiconductors, Chinese Academy of Sciences, P.O. Box 912, Beijing 100083, China

(Dated: November 10, 2018)

We demonstrate theoretically that electric field can drive a quantum phase transition between band insulator to topological insulator in CdTe/HgCdTe/CdTe quantum wells. The numerical results suggest that the electric field could be used as a switch to turn on or off the topological insulator phase, and temperature can affect significantly the phase diagram for different gate voltage and compositions. Our theoretical results provide us an efficient way to manipulate the quantum phase of HgTe quantum wells.

PACS numbers: 73.43.Nq, 72.25.Rb, 73.61.Ga, 74.62.-c

Topological insulator (TI) is a very recent discovery and has attracted a rapid growing interests due to its novel transport property<sup>1,2,3,4</sup>. Topological insulators possess a gap in the bulk but a gapless edge states at its boundary, therefore display remarkable transport property due to the presence of the topological edge states, e.g., quantum spin Hall effect (QSHE). The QSHE is protected by the time-reversal symmetry and robust against the local perturbation, e.g., impurity scattering. Searching for new TI becomes a central issue in this rapid growing field. Recently, the HgTe QWs have been demonstrated to be a 2D TI to exhibit the QSHE<sup>3</sup> and BiSb alloys have been proven to be a 3D TI with a conducting surface<sup>5</sup>. A few other materials, such as InAs/GaSb QWs, BiSe, BiTe and SbTe alloys<sup>6</sup>, are also predicted to be TIs and demonstrated experimentally. Besides finding new TI materials, searching the ways to drive a band insulator (BI) into a topological insulator is also important. It has been demonstrated to be possibly realized by tuning the thickness of HgTe QW. However, tuning the thickness of QW is not a convenient way to drive the phase transition. Therefore other efficient ways such as external fields and temperature is highly desirable to drive a BI into a TI. These ways would be very important for both potential device applications and basic physics.

In this Letter, we demonstrate theoretically that a BI can be driven into a TI by tuning external electric field in CdTe/Hg<sub>1-x</sub>Cd<sub>x</sub>Te/CdTe QWs based on the self-consistent calculation of the eight-band Kane model and the Poisson equation. We demonstrate electric field can change the interband coupling significantly and consequently leads to strong variations of the band structures, i.e., therefore leads to the quantum phase transition from a BI to a TI. We also show phase diagrams at plenty of parameters and consider the temperature effect on the phase transition. One can see that the critical gate voltage of external phase transition can be reduced at high temperature, small Cd composition and thick thickness of well. Our results could be useful in finding the optimized parameters to realize the phase transition in experiment.

We consider a CdTe/Hg<sub>1-x</sub>Cd<sub>x</sub>Te/CdTe QW grown along the [001] direction [see Fig. 1 (a)]. The axis  $x$ ,  $y$ , and  $z$  is chosen to be along [100], [010], and [001], respectively. Within the envelope function approximation, the Kane model

is a good starting point for systems with strong interband coupling. When an external voltage is applied perpendicular to the quantum well plane (at the two sides of the QW), electrons

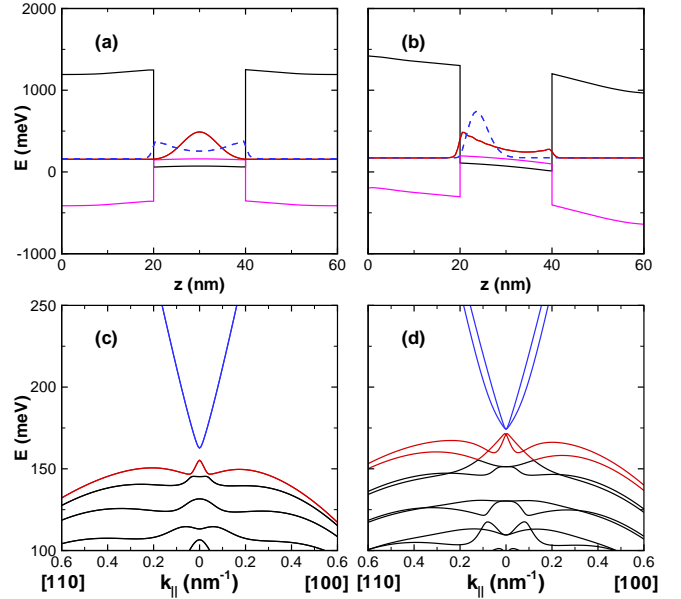


FIG. 1: (Colour online) Self-consistently calculated band profiles ( $T = 0$  K) (a) and energy dispersion (c) of a symmetrically doped CdTe (20 nm)/Hg<sub>0.88</sub>Cd<sub>0.12</sub>Te (20 nm)/CdTe (20 nm) QW without external gate voltage. (b) and (d) are the same as (a) and (c) but with gate voltage  $U_{ex} = 0.5$  V between the top and bottom gates. The red solid and blue dashed curves in Fig. 1(a) and 1(b) denote the probability distributions of the states of the highest valence subband and lowest conduction subband, respectively. The doping density is  $N_d = 5 \times 10^{11} \text{ cm}^{-2}$ .

inside the QW will redistribute due to the effect of the electric field. The charge redistribution induces an internal electric field, which affects the charge density distribution, therefore we need to solve the eight-band Kane model and the Poisson equation self-consistently.

The Kane Hamiltonian for zinc-blende crystals near the  $\Gamma$  point can be written as

$$H_k = \begin{bmatrix} A & 0 & i\sqrt{3}V^\dagger & \sqrt{2}U & iV & 0 & iU & \sqrt{2}V \\ 0 & A & 0 & -V^\dagger & i\sqrt{2}U & -\sqrt{3}V & i\sqrt{2}V^\dagger & -U \\ -i\sqrt{3}V & 0 & -(P+Q) & L & M & 0 & \frac{i}{\sqrt{2}}L & -i\sqrt{2}M \\ \sqrt{2}U & -V & L^\dagger & -(P-Q) & 0 & M & i\sqrt{2}Q & i\sqrt{\frac{3}{2}}L \\ -iV^\dagger & -i\sqrt{2}U & M^\dagger & 0 & -(P-Q) & -L & -i\sqrt{\frac{3}{2}}L^\dagger & i\sqrt{2}Q \\ 0 & -\sqrt{3}V^\dagger & 0 & M^\dagger & -L^\dagger & -(P+Q) & -i\sqrt{2}M^\dagger & -\frac{i}{\sqrt{2}}L^\dagger \\ -iU & -i\sqrt{2}V & -\frac{i}{\sqrt{2}}L^\dagger & -i\sqrt{2}Q & i\sqrt{\frac{3}{2}}L & i\sqrt{2}M & -P-\Delta & 0 \\ \sqrt{2}V^\dagger & -U & i\sqrt{2}M^\dagger & -i\sqrt{\frac{3}{2}}L^\dagger & -i\sqrt{2}Q & \frac{i}{\sqrt{2}}L & 0 & -P-\Delta \end{bmatrix} \quad (1)$$

where

$$A = E_v + E_g + \mathbf{k}A_c\mathbf{k}, \quad (2a)$$

$$P = -E_v + \frac{\hbar^2}{2m_0}\mathbf{k}\gamma_1\mathbf{k}, \quad (2b)$$

$$Q = \frac{\hbar^2}{2m_0}(k_x\gamma_2k_x + k_y\gamma_2k_y - 2k_z\gamma_2k_z), \quad (2c)$$

$$L = i\frac{\sqrt{3}\hbar^2}{m_0}\{k_- \gamma_3 k_z\}, \quad (2d)$$

$$M = -\frac{\sqrt{3}\hbar^2}{2m_0}[k_x\gamma_2k_x - k_y\gamma_2k_y - 2i\{k_x\gamma_3k_y\}], \quad (2e)$$

$$U = \frac{1}{\sqrt{3}}P_0k_z, \quad (2f)$$

$$V = \frac{1}{\sqrt{6}}P_0k_-. \quad (2g)$$

where  $\mathbf{k} = (\mathbf{k}_\parallel, -i\partial/\partial z)$ ,  $k_\pm = k_x \pm ik_y$ , and  $\{k_\alpha\gamma_k\beta\} = (k_\alpha\gamma_k\beta + k_\beta\gamma_k\alpha)/2$  ( $\alpha, \beta = x, y, z$ ). Here the in-plane momentum is a constant of motion and can be replaced by its eigenvalue  $\mathbf{k}_\parallel$ . The total Hamiltonian becomes  $H(\mathbf{k}_\parallel) = H_k(\mathbf{k}_\parallel) - eV_{in}(z) + eV_{ex}(z)$ .

The subband dispersions and the corresponding eigenstates are obtained from the Schrödinger equation

$$H(\mathbf{k}_\parallel) |\Psi_s(\mathbf{k}_\parallel)\rangle = E_s(\mathbf{k}_\parallel) |\Psi_s(\mathbf{k}_\parallel)\rangle, \quad (3)$$

where  $s$  is the index of the subband and  $|\Psi_s(\mathbf{k}_\parallel)\rangle = \exp(i\mathbf{k}_\parallel \cdot \boldsymbol{\rho})[\varphi_1^s(z), \varphi_2^s(z), \dots, \varphi_8^s(z)]^T$  is the envelope function. We solve the Schrödinger equation by expanding  $\varphi_n^s$  by a series of plane waves<sup>13</sup>. In our calculation,  $N \approx 30$  is good enough to get convergent results.

The internal electrostatic potential  $V_{in}(z)$  is determined by the Poisson equation

$$\frac{d}{dz}\varepsilon(z)\frac{d}{dz}V_{in}(z) = \rho_h(z) - \rho_e(z) + N_dD(z), \quad (4)$$

where  $\rho_e(z)$  and  $\rho_h(z)$  are, respectively, the charge density of electrons and holes and  $\varepsilon(z)$  is the static dielectric constant.  $N_d$  is the ionized donors density and  $D(z)$  is the distribution function of the impurities. In this paper,  $D(z)$  is

TABLE I: Band structure parameters of  $\text{Hg}_{1-x}\text{Cd}_x\text{Te}$ <sup>10</sup> and  $\text{CdTe}$ <sup>11</sup> used in the Kane Hamiltonian.

	$E_g$ (eV)	$\Delta$ (eV)	$E_p$ (eV)	$F$	$\gamma_1$	$\gamma_2$	$\gamma_3$	$\varepsilon$
$\text{Hg}_{1-x}\text{Cd}_x\text{Te}$		1.0	19.0	-0.8	3.3	0.1	0.9	21
$\text{CdTe}$	1.606	0.91	18.8	-0.09	1.47	-0.28	0.03	10.4

assumed to be an exponentially decayed function. For simplicity, we take  $T = 0$  K and the axial approximation in the self-consistent procedure. The Fermi level  $E_F$  is determined by the charge neutrality condition  $\int_0^L [\rho_e(z) - \rho_h(z)] dz = N_d$ , where  $L = L_{\text{HgCdTe}} + 2L_{\text{CdTe}}$  is the total width of barriers and QW. The thickness of  $\text{CdTe}$  barrier  $L_{\text{CdTe}}$  is fixed at 20 nm.

While the external electrostatic potential  $V_{ex}(z)$  can be determined by

$$\frac{d}{dz}\varepsilon(z)\frac{d}{dz}V_{ex}(z) = 0, \quad (5)$$

and the boundary condition

$$\int_0^L \varepsilon(z)\frac{d}{dz}V_{ex}(z) = \varepsilon_0 U_{ex}. \quad (6)$$

$U_{ex}$  is the external voltage which could be applied on the top and bottom gate at the two sides of the QW.

In Table I we list the band parameters used in our calculation<sup>10,11</sup>. The Kane parameters of  $\text{Hg}_{1-x}\text{Cd}_x\text{Te}$  can be assumed to be  $x$ -independent<sup>10</sup>, since the band structure dependence on the Cd composition  $x$  caused mainly by the variation of the band gap  $E_g$ . And the band gap  $E_g$  of  $\text{Hg}_{1-x}\text{Cd}_x\text{Te}$  can be obtained in the previous work<sup>12</sup>.

In Figs. 1 (a) and 1(b) we show the self-consistently calculated band profiles of  $\text{CdTe}/\text{Hg}_{0.88}\text{Cd}_{0.12}\text{Te}/\text{CdTe}$  QW with and without external electric field. The strong inter-band coupling makes the quantum states near the gap in  $\text{CdTe}/\text{Hg}_{1-x}\text{Cd}_x\text{Te}/\text{CdTe}$  QWs very different from those in conventional semiconductor QWs. This can be seen clearly from the wavefunction distributions of carriers. For the normal band structure, the probability of the highest valence sub-

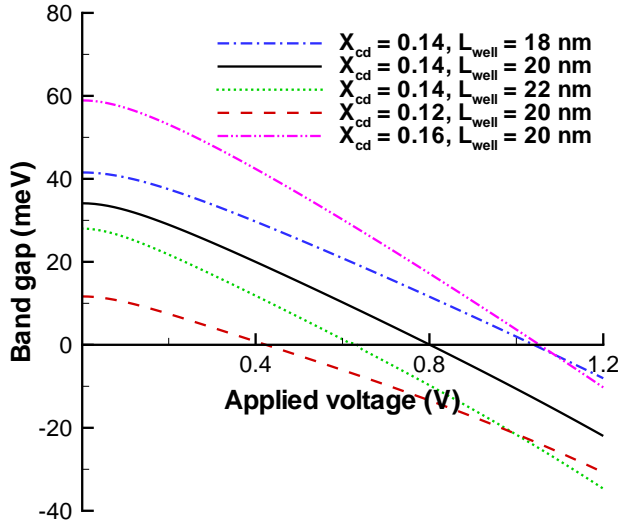


FIG. 2: (Colour online) Bandgap of CdTe/Hg<sub>1-x</sub>Cd<sub>x</sub>Te/CdTe QW ( $T = 0$  K) as a function of external gate voltage for different thickness of Hg<sub>1-x</sub>Cd<sub>x</sub>Te well and the composition of Cd in Hg<sub>1-x</sub>Cd<sub>x</sub>Te alloy.

band state localizes at the center of the QW, while the probability of lowest conduction subband state is more localized in the vicinity of the sides of the QW (see the red solid and blue dashed curves in Fig. 1 (a)). This is because the main component of the lowest conduction subband state for the normal band structure is electron and it couples strongly with the light-hole component even at  $\mathbf{k}_{\parallel} = 0$ , while the main component of the highest valence subband state is heavy-hole and it decouples with the other components at  $\mathbf{k}_{\parallel} = 0$ . When an external gate voltage is applied, the band structure changes from the normal band structure to the inverted band structure, and the probability distributions of the lowest conduction subband and highest valence subband states exchange (see the red and blue curves in Fig. 1 (b)). In Figs. 1(c) and (d) we plot the corresponding band structures of CdTe/Hg<sub>1-x</sub>Cd<sub>x</sub>Te/CdTe QWs with and without electric field. We demonstrate clearly that electric field can change the interband coupling significantly and consequently leads to strong variations of the band structures, i.e., the variation from the normal band structure to the inverted band structure. Due to the enhanced interband coupling, the lowest conduction subbands and the highest valence subbands exhibit a strong anticrossing behavior and open a mini hybridized gap at a finite  $\mathbf{k}_{\parallel}$  in the case of the inverted band structure. The edge states will appear if a lateral confinement is applied to this QW with the inverted band structure. Our numerical results demonstrate that a normal insulator indeed can be driven into a topological insulator electrically.

Next, we turn to discuss how electric fields affect the bandgap of QWs. Fig. 2 shows that the bandgap of CdTe/Hg<sub>1-x</sub>Cd<sub>x</sub>Te/CdTe QW as a function of the external gate voltage for QWs with different thicknesses of well and Cd compositions. In thin CdTe/Hg<sub>1-x</sub>Cd<sub>x</sub>Te/CdTe QWs with

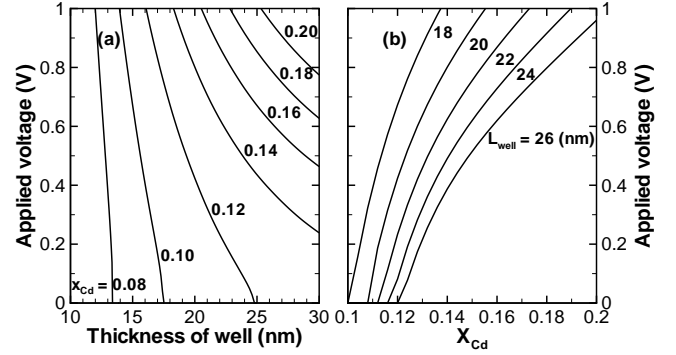


FIG. 3: The critical gate voltage as function of (a) the thickness of well and (b) the composition of Cd for different CdTe/Hg<sub>1-x</sub>Cd<sub>x</sub>Te/CdTe QWs at  $T = 0$  K.

out external electric fields, the quantum confinement effect can push the lowest conduction subbands to higher energy and therefore the QW exhibits the normal band structure. From this figure, one can see clearly that for a certain Cd composition and thickness of well, the bandgap of QW can be reduced into the negative value by tuning external voltages. Increasing the Cd composition or decreasing the thickness of the Hg<sub>1-x</sub>Cd<sub>x</sub>Te well, the band gap of unbiased CdTe/Hg<sub>1-x</sub>Cd<sub>x</sub>Te/CdTe QW would be enlarged so one needs larger gate voltage to drive this band insulator to the topological insulator.

In Fig. 3 (a) we plot the phase diagram as function of the gate voltage (equivalently electric field) and the thickness of QWs for different compositions of Cd atoms at  $T = 0$  K. For a given QW with a fixed Cd composition and thickness of QW, a quantum phase transition between a BI and a TI takes place when the applied voltage is larger than a critical voltage. One see that higher voltage is needed to induce the transition in narrow QWs for a fixed composition. For a fixed thickness of the QW, the transition is more easily induced at small compositions. Fig. 3 (b) displays the phase diagram as function of the gate voltage and the Cd compositions. With increasing the external voltage, the QSH states can even be found for high composition  $x$ . For wider QWs, one can see that it is more easily to drive a normal band insulator into a topological insulator. From Fig. 3, we find that the thickness of well to maintain the QW in topological insulator phase can not be less than 13 nm when the Cd composition in Hg<sub>1-x</sub>Cd<sub>x</sub>Te well is smaller than 0.08, and hardly possible to see the quantum phase transition driven by external electric field since the boundary of phase diagram almost does not change with increasing the gate voltage. Notice that a very large electrical field can also lead to the leaky of electrons out of the QWs because of quantum confinement of QW.

Finally, we will discuss the temperature effect on the transition between the BI and the TI. Since the bulk bandgap of Hg<sub>1-x</sub>Cd<sub>x</sub>Te varies with increasing temperature, the phase diagram will be very different from that at  $T = 0$ . Fig. 4 (a) shows the critical thickness of well of the phase transition increase rapidly (without external gate voltage) with increasing

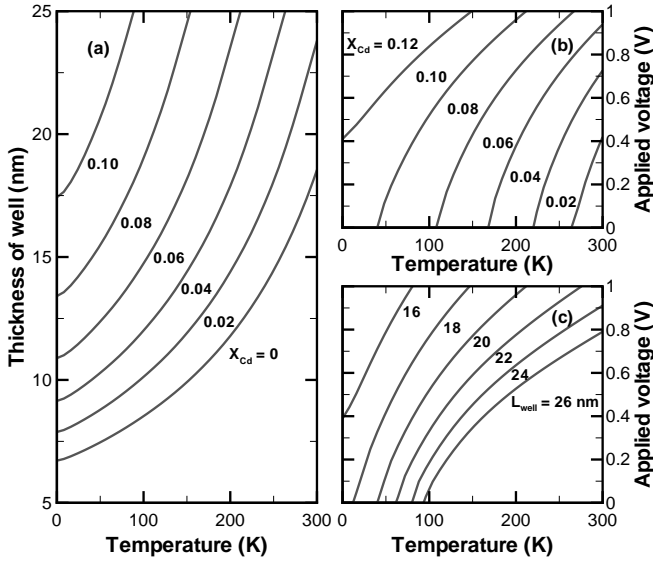


FIG. 4: (a) The critical thickness of well as function of temperature for CdTe/Hg<sub>1-x</sub>Cd<sub>x</sub>Te/CdTe QWs with different Cd composition without external gate voltage. (b) The critical gate voltage as function of temperature for QWs with fixed thickness (20 nm well) and different Cd composition. The same as (b) but for QWs with fixed Cd composition  $x = 0.10$  and different thickness of well.

temperature. Take the CdTe/HgTe/CdTe QW ( $x = 0$ ) for ex-

ample, the thickness of the QW varies from 6.7 nm to 18.5 nm when temperature increase from 0 K to 300 K. Such great change indicates that temperature is a significant factor of the phase transition between BI and the TI in these QWs. Fig. 4 (b) and (c) shows that the critical voltage would increase with increasing temperature for QWs with fixed Cd compositions and thickness of well. Decreasing the Cd composition or increasing the thickness of well would make the phase transition possibly occurs at higher temperature and smaller gate voltage. One can see from the panel (b) that at  $T = 300$  K, it is possible to drive a CdTe/Hg<sub>1-x</sub>Cd<sub>x</sub>Te/CdTe QW with  $x = 0.02$  and 20 nm well width at the voltage between the top and bottom gates  $U_{ex} = 0.4$  V.

We demonstrate theoretically that external electric field and temperature can drive a quantum phase transition between a band insulator and a topological insulator in CdTe/Hg<sub>1-x</sub>Cd<sub>x</sub>Te/CdTe quantum wells. It provides us an efficient way to drive the band insulator into the topological insulator. Our theoretical result is interesting both from the basic physics and potential application of the spintronic devices based on this novel topological insulator system.

#### Acknowledgments

This work was supported partly by the NSFC Grant Nos. 60525405 and 10874175, and the bilateral program between China and Sweden.

- <sup>1</sup> C. L. Kane and E. J. Mele, Phys. Rev. Lett. **95**, 226801 (2005).
- <sup>2</sup> B. A. Bernevig, T. L. Hughes, and S. C. Zhang, Science **314**, 1757 (2006).
- <sup>3</sup> M. König, S. Wiedmann, C. Brune, A. Roth, H. Buhmann, L. W. Molenkamp, X. L. Qi, and S. C. Zhang, Science **318**, 766 (2007).
- <sup>4</sup> L. Fu, C. L. Kane, and E. J. Mele, Phys. Rev. Lett. **98**, 106803 (2007).
- <sup>5</sup> D. Hsieh, Y. Xia, L. Wray, D. Qian, A. Pal, J. H. Dil, J. Osterwalder, F. Meier, G. Bihlmayer, C. L. Kane, Y. S. Hor, R. J. Cava, M. Z. Hasan, Science **323**, 919 (2009).
- <sup>6</sup> H. Zhang, C. X. Liu, X. L. Qi, X. Dai, Z. Fang, and S. C. Zhang, Nat. Phys. **5**, 438 (2009).
- <sup>7</sup> Y. A. Bychkov and E. I. Rashba, J. Phys. C **17**, 6039 (1984).
- <sup>8</sup> W. Yang, Kai Chang, and S. C. Zhang, Phys. Rev. Lett. **100**, 056602 (2008).
- <sup>9</sup> M. G. Burt, J. Phys.: Condens. Matter **4**, 6651 (1992); B. A. Foreman, Phys. Rev. B **56**, R12748 (1997); T. Darnhofer and U. Rossler, *ibid.* **47**, 16020 (1993).
- <sup>10</sup> *II-VI and I-VII Compounds; Semimagnetic Compounds*, edited by Landolt-Börnstein, Group III Vol. 41B, edited by U. Rössler (Springer-Verlag, Berlin, 1999).
- <sup>11</sup> X. C. Zhang, A. Pfeuffer-Jeschke, K. Ortner, V. Hock, H. Buhmann, C. R. Becker, and G. Landwehr, Phys. Rev. B **63**, 245305 (2001).
- <sup>12</sup> C. R. Becker, V. Latussek, A. Pfeuffer-Jeschke, G. Landwehr, and L. W. Molenkamp, Phys. Rev. B **62**, 10353 (2000).
- <sup>13</sup> W. Yang and Kai Chang, Phys. Rev. B **72**, 233309 (2005).
- <sup>14</sup> R. Winkler, *Spin-Orbit Coupling Effects in Two-Dimensional Electron and Hole Systems*, (Springer-Verlag, Berlin, 2003), Chap. 3, pp. 29-33.
- <sup>15</sup> W. Yang and Kai Chang, Phys. Rev. B **74**, 193314 (2006).